2016 International Symposium on Nonlinear Theory and Its Applications,
NOLTA2016, Yugawara, Japan, November 27th-30th, 2016

A Variety of Super-Stable Periodic Orbits in a Simple Dynamical System with Integrate-and-Fire Switching

Risa Takahashi† and Toshimichi Saito†

†Department of Electronics and Electrical Engineering, Hosei University
3–7–2 Kajino-cho, Koganei, Tokyo 184-8584, Japan
Emails: risa.takahashi.3j@stu.hosei.ac.jp; tsaito@hosei.ac.jp

Abstract—This paper studies dynamics of a simple switched dynamical system. Repeating integrate-and-fire behavior between a constant threshold and piecewise linear periodic base signal, the system can exhibit a variety of chaotic and super-stable periodic orbits. The dynamics is simplified into a piecewise linear return map. Using the return map, parameter conditions of various super-stable periodic orbits are analyzed precisely.

1. Introduction

This paper studies a variety of super-stable periodic orbits in a simple switched dynamical system (SDS [1]-[3]). The dynamics of SDS is based on integrate-and-fire behavior between a constant threshold signal and periodic base signal. Especially, we consider the case where the base signal given by addition of the first triangular signal with period T and the second triangular signal with period T/M. If the base signal is given by either the first of second signal only, the SDS exhibits chaotic orbit characterized by positive Lyapunov exponent. However, if the base signal is given by both the first and second signal, the SDS exhibits a variety of super-stable periodic orbit (SSPO) such that almost all initial state fall rapidly into the SSPO.

The dynamics of SDS is integrated into a piecewise linear return map. Based on the map, we present simple and systematic calculation methods of parameter regions of the SSPOs. We then clarify that, a variety of SSPOs exists or co-exist in the parameter space. Although discussion of this paper is based on theory-based numerical experiments, we have prepared laboratory measurements of typical phenomena for the final version.

The SDS is inspired by a simple integrate-and-fire type spiking neuron model [1]-[6]. Analysis results of simple neuron models have contributed to consideration of neural information processing function [7] [8]. Engineering applications of such systems are many, including signal/image processing and ultra wide band communication [9] [10]. Analysis of such systems is important not only as a nonlinear dynamical system but also for engineering applications.

It should be noted that our previous paper [3] has discussed SSPOs, however has not discussed parameter regions of various SSPOs and their calculation method.

2. Circuit Model

Figures 1 and 2 show a circuit model and dynamics of the SDS, respectively. The capacitor voltage v rises to the threshold V_T with slope s. As v reaches the threshold then the SDS outputs a spike $Y(t) = E$ and v reset to the periodic base signal($B(t)$) with period T. Repeating this integrate-and fire behavior, the SDS outputs spike-train $Y(t)$. For simplicity, the inner resistors are ignored ($r_1 \to \infty, r_2 \to 0$) and the switching is assumed to be ideal: v_1 is reset instantaneously without delay. The dynamics is described by

$$\begin{cases} C\dfrac{dv}{dt} = I, & Y(t) = -E \quad \text{for } v(t) < V_T \\ v(t_+) = B(t_+), & Y(t_+) = E \quad \text{if } v(t) = V_T \end{cases} \tag{1}$$

$$B(t) = K_1 B_1(t) + K_3 B_1(3t) + E_0,\ B_1(t+T) = B_1(t) \tag{2}$$

$$B_1(t) = \begin{cases} -(A-2)t/T & \text{for } -d < t/T < d \\ A(t/T - 2d) + 2d & \text{for } d < t/T < 1-d \end{cases} \tag{3}$$

where $B(t) < V_T$. Using dimensionless variables and parameters:

$$\begin{gathered} \tau = \frac{t}{T},\ x = \frac{v}{V_T},\ \dot{x} = \frac{dx}{d\tau},\ y = \frac{Y+E}{2} \\ k_1 = \frac{K_1}{V_T},\ k_3 = \frac{K_3}{V_T},\ a_0 = \frac{E_0}{V_T},\ s = \frac{IT}{CV_T} \end{gathered} \tag{4}$$

Eqs. (1)-(4) are transformed into

$$\begin{cases} \dot{x} = s & \text{for } x < 1 \\ x(\tau_+) = b(\tau_+) & \text{if } x(\tau) = 1 \end{cases} \tag{5}$$

$$b(\tau) = k_1 b_1(\tau) + k_3 b_1(3\tau) + a_0,\ b_1(\tau+1) = b_1(\tau) \tag{6}$$

$$b_1(\tau) = \begin{cases} -(A-2)\tau & \text{for } -d < \tau < d \\ A(\tau - 2d) + 2d & \text{for } d < \tau < 1-d \end{cases} \tag{7}$$

where $\dot{x} \equiv dx/d\tau$. The base signal is characterized by parameters A and d. For simplicity, we assume

$$2 < A < 4,\ \ 0 < d < 0.5$$

In this paper, we consider three cases of the $b(\tau)$.

Case 1: The first component only ($k_1 \neq 0, k_3 = 0$)

Case 2: The second component only ($k_1 = 0, k_3 \neq 0$)

Case 3: Two inputs ($k_1 \neq 0, k_3 \neq 0$)

It goes without saying that the theorem of superposition is not valid in this nonlinear system.

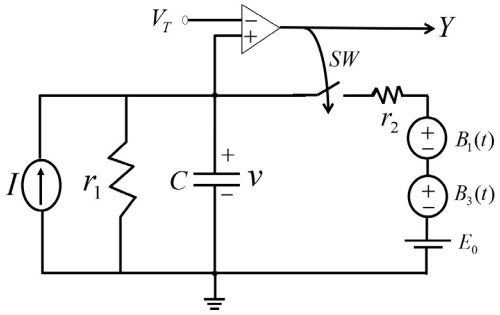

Figure 1: A circuit model

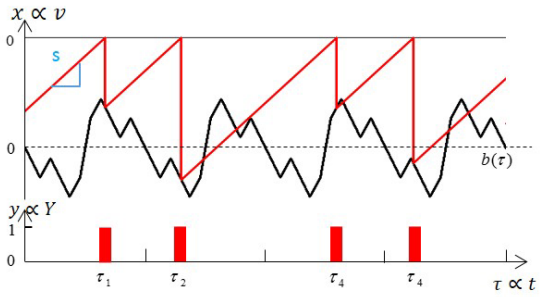

Figure 2: Example waveforms

3. Experiments

In order to confirm typical phenomena, we have fabricated a breadboard prototype of the BN. Figure 3 shows typical phenomena. The BN exhibits chaos for $B(t) = B_1(t)$ (first component only) or $B(t) = B_3(t)$ (second component only). However, if $B(t) = B_1(t) + B_3(t)$ then the BN exhibits periodic waveform as shown in Fig. 3(c). That is, chaotic behavior of each BN can be changed into periodic behavior by the two inputs.

4. Spike-phase Map

In order to analyze the dynamics, we derive a SPmap of the SDS. Let τ_n denote the n-th spike position. Since τ_{n+1} is determined by τ_n, we can define the Smap.

$$\tau_{n+1} = \tau_n + (1 - b(\tau_n))/s \equiv F(\tau_n) \tag{8}$$

Since $F_1(\tau + 1) = F_1(\tau) + 1$ is satisfied, we introduce the phase variable $\theta_1(n) = \tau_1 \bmod 1$. Using this, we can define the Pmap as shown in Fig. 4:

$$\theta_{n+1} = f(\theta_n) \equiv F(\theta_n) \bmod 1 \tag{9}$$

Substituting $k_3 = 0$ and $a_0 = 0$ into Eq. (6), we obtain the Pmap for the first component. Substituting $k_1 = 0$ into Eq. (6), we obtain the Pmap for the second component.

$$f(\theta_n) = \begin{cases} a\theta & \text{for } -d < \theta < d \\ -a\theta + (1+a)/2 & \text{for } d < \theta < 1 - d \end{cases} \tag{10}$$

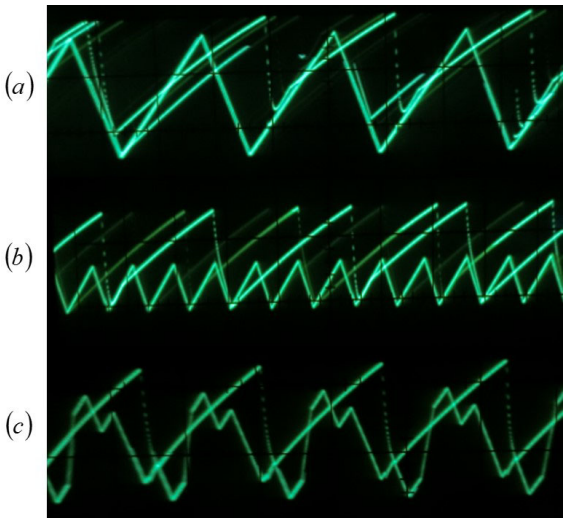

Figure 3: Typical waveforms of BN. ($T = 1.0$[ms], $C = 0.022$[μF], $r_1 = 120.2$[kΩ], $r_2 = 1.1$[kΩ], $V_T = 1$[V], $A = 4.0$, $d = 0.33$, $E_0 = 0$) (a)first component only ($k_1 = 1$, $k_3 = 0$), (b)second component only ($k_1 = 0, k_3 = \frac{1}{3}$), (c)two inputs ($k_1 = 1$, $k_3 = \frac{1}{3}$).

The shape of the Pmap depends on the shape of $b(\tau)$. As the parameter varies, the shape of Pmap varies and SDS can exhibit various spike-trains. Since the base signal is piecewise linear, the maps are also piecewise linear and precise numerical analysis is possible.

In Case 1 and 2, the Pmap exhibits chaos as shown in Fig. 5(a) and (b). In Case 3, the Pmap exhibits super-stable periodic orbit(SSPO) as shown in Fig. 6. That is, chaotic behavior of each SDS whose base signal is given by single component can be changed into periodic behavior by the two inputs.

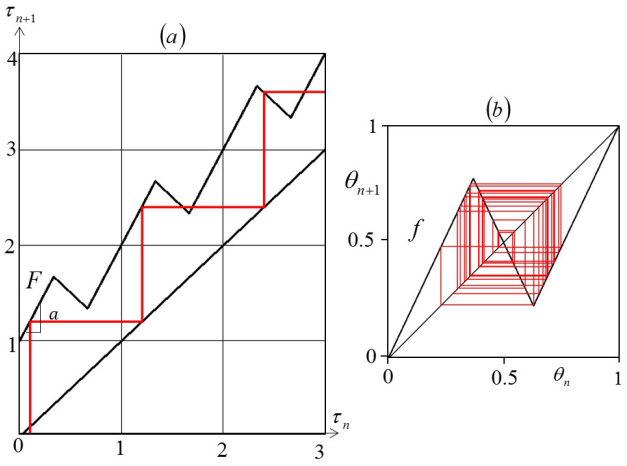

Figure 4: (a) Spike-position map(Smap), (b) Spike-phase map(Pmap).

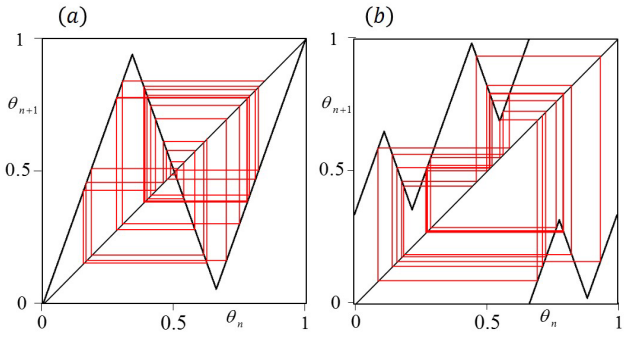

Figure 5: Pmap for $a_0 = 0.34$, $a = 2.77$. (a) The first component only ($k_1 = 1, k_3 = 0$), (b) The second component only ($k_1 = 0, k_3 = 1/3$).

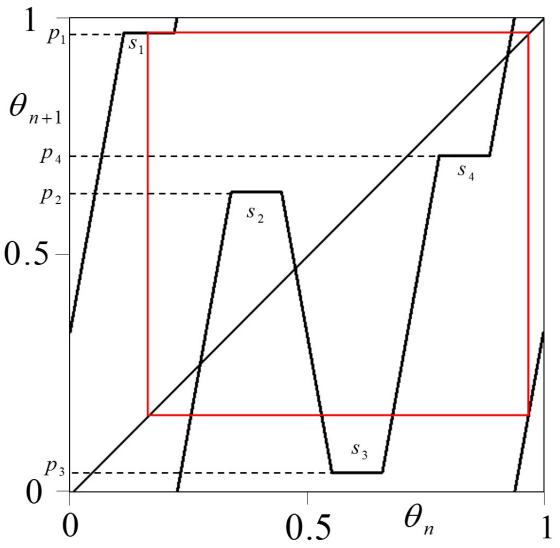

Figure 6: Pmap for $k_1 = 1, k_3 = 1/3$, $a_0 = 0.34$, $a = 2.77$.

5. Analysis

First, we give several basic definitions. A point $\theta_f \in I$ is said to be a 1-periodic point or fixed point if $F(\theta_f) = \tau_f$. A point $\theta_p \in I$ is said to be a k-periodic point if $F^k(\theta_p) = \theta_p$ and $F^l(\theta_p) \neq \theta_p$ for $1 \leq l \leq k$ where F^k is the k-fold composition of F and $k \geq 2$.

Now we consider the periodic behavior in Case 3. Fig. 7 shows several Pmaps. Corresponding SDS exhibits periodic waveform with period 2. Note that the Pmap has four segments with zero-slope(s_1 to s_4) and exhibit super-stable periodic orbits (SSPO). Let points p_1 to p_4 denote images of s_1 to s_4 as shown in Fig. 6.

We explain an outline of the analysis. First, since the Pmap includes four segments with slope-zero and other segments are expanding, a trajectory started from one of the four points p_1 to p_4 must return to either of the four points. That is, it is sufficient to use one of the four point as an initial values. If a trajectory started from p_i ($i = 1 \sim 4$) returns to p_i then the orbit is SSPO. If a trajectory started from p_i falls into $p_j (j \neq i)$ then orbit is transient to some SSPO.

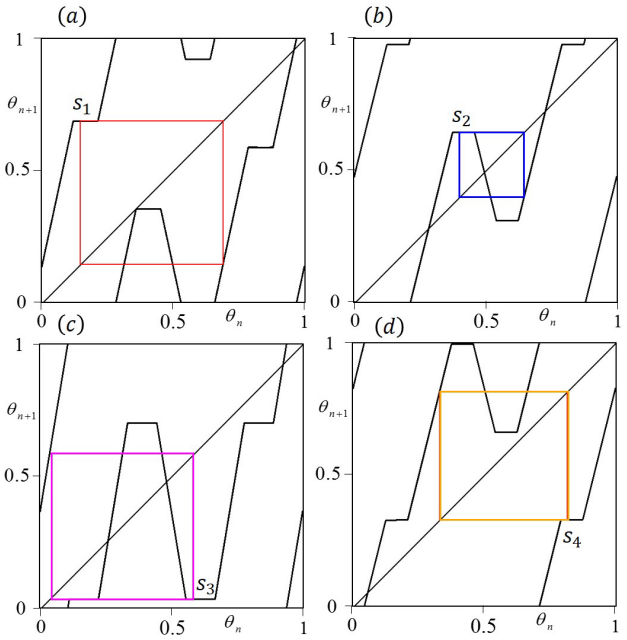

Figure 7: Pmap for two inputs($k_1 = 1, k_3 = 1/3$). (a) $a_0 = 0.14$, $a = 2.3$, (b) $a_0 = 0.50$, $a = 2.4$, (c) $a_0 = 0.37$, $a = 3.0$, (d) $a_0 = 0.83$, $a = 2.3$.

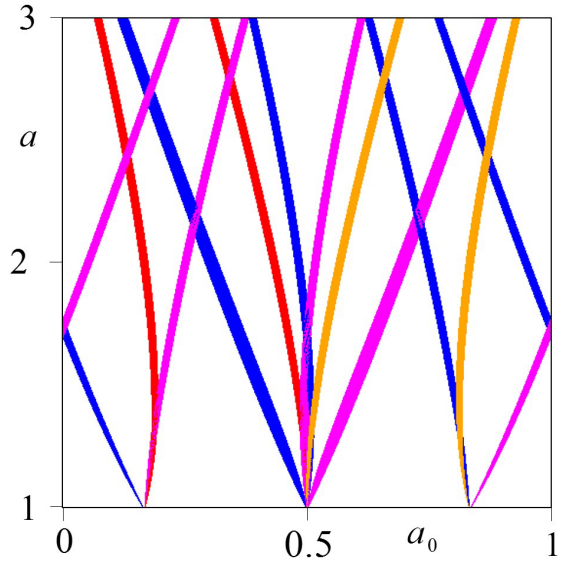

Figure 8: Parameter regions for super-stable periodic spike-train with period 2. $(k_1, k_3) = (1, 1/3)$ and $d = \frac{1+a}{4a}$. Red region: SSPO started from s_1. Blue region: SSPO started from s_2. Pink region: SSPO started from s_3. Orange region: SSPO started from s_4.

Fig. 7 shows typical Pmaps of SSPOs with period 2. Fig. 8 shows parameter regions for SSPO with period 2: a basic

results of the bifurcation analysis in the $a_0 - a$ plane. It is derived by the following 3 steps.

Step 1: Select the dc component $a0$ and the slope a as control parameters.

Step 2: Use p_i ($i = 1 \sim 4$) as an initial values.

Step 3: If a trajectory return to p_i by twice then plot to the $a_0 - a$ plane.

After the step is terminated, we obtain parameter regions for SSPO with period 2.

6. Conclusions

We have studied a variety of super-stable periodic orbits in a simple dynamical system with integrate-and fire switching. Using Pmaps, we have calculated parameter regions of various SSPOs. The future problem includes detailed analysis of typical bifurcation phenomena and application to spike-based engineering systems.

References

[1] H. Torikai and T. Saito, Return map quantization from an integrate-and-fire model with two periodic inputs, IEICE Trans. Fundamntals, E82-A, 7, pp. 1336-1343, 1999.

[2] Y. Kon'no, T. Saito, and H. Torikai, Rich dynamics of pulse-coupled spiking neurons with a triangular base signal, Neural Networks, 18, pp. 523-531, 2005.

[3] R. Takahashi, Y. Yanase, and T. Saito, Analysis of various super-stable periodic spike-trains in bifurcating neuron with two triangular inputs, Proc. of NOLTA, pp. 177-180, 2015.

[4] R. Perez and L. Glass, Bistability, period doubling bifurcations and chaos in a periodically forced oscillator. Phys. Lett., 90A, 9, pp. 441-443, 1982.

[5] G. Lee and N. H. Farhat, The bifurcating neuron network 1. Neural networks, 14, pp. 115-131, 2001.

[6] E. D. M. Hernandez, G Lee, and N. H. Farhat, Analog realization of arbitrary one-dimensional maps, IEEE Trans. Circuits Syst. I, 50, 12, pp. 1538-1547, 2003.

[7] E. M. Izhikevich, Simple model of spiking neurons, IEEE Trans. Neural Networks, 14, 6, pp. 1569-1572, 2003.

[8] N. Ning, H. Kejie and S. Luping, Artificial neuron with somatic and axonal computation units: mathematical and neuromorphic models of persistent firing neurons, Proc. of IEEE-INNS/IJCNN, pp. 473-479, 2012.

[9] S. R. Campbell, D. Wang, and C. Jayaprakash, Synchrony and desynchrony in integrate-and fire oscillators. Neural Computation 11, 1595-1691, 1999.

[10] N. F. Rulkov, M. M. Sushchik, L. S. Tsimring and A. R. Volkovskii, Digital communication using chaotic-pulse-position modulation. IEEE Trans. Circuits Systs., I 48(12), 1436-1444, 2001.